The effect of insoluble salts in bituminized waste products leached in pure water

H. Jaffel [1,3], A. Guillermo [2], O. Diat [1], A.Ledieu [3], A. Poulesquen [3]

[1] *ICSM – UMR CNRS 5257 – CEA Marcoule*
[2] *SPrAM – UMR CNRS 5819 – CEA Grenoble*
[3] *DEN/DTCD – CEA Marcoule*
olivier.diat@cea.fr

Abstract *– Our aim is to refine the current description of the leaching phenomenology with cross-linked characterizations of Bituminized Waste Products in contact with water, at the early stages of the leaching as well as the longer ones. For that sake, three model BWP have been synthesised, varying the chemical content of salts and the grain size distribution. Water sorption, ^{1}H CPMG NMR techniques are the main techniques used for this study. They have been compared to the kinetics of water uptake in leaching experiments.*

INTRODUCTION

In France, bitumen is used since four decades as a container material for low/intermediate activity and long lifetime radionuclides. Industrial Bituminized Waste Products (BWP) are produced by continuous extrusion of 60 %w. of bitumen and 40%w. of salts (volumic ratio ~3:1), in which a very small fraction is lastly radioactive. The prediction of long term behaviour, needed for a sustainable management of BWP, is usually achieved by studying the leaching of non radioactive-model materials. Previous studies have allowed the implementation of models, able to predict the experimental water uptake and ionic releases due to leaching, as a function of inputs such as the proportion of soluble species incorporated in BWP and the nature of the leachant [1,2].
In that context, this work is a contribution to the deeper investigation of the leaching phenomenology, with a special focus on the role of the insoluble species.

DESCRIPTION OF MATERIALS

Three synthetic and inactive BWP have been studied varying the chemical composition of incorporated salts. All have been produced in the same conditions with respect to the extrusion process [3], using the same bitumen composition (Azalt 70/100). Table 1 give the main parameters related to the chemical composition of produced materials. A-type BWP composition is to be considered as representative for industrial materials and B- and C-types are simplified model materials.
The figure 1 shows the pristine microstructure of samples A and B, as observed with environmental scanning electron microscope. ESEM observations have been performed in CEA Cadarache (DEC/SA3C/LARC).

TABLE I. Chemical composition of BWP samples.

Ref of BWP samples	Salts content (%w.)	Water content (%w.)	Incorporated salts (%w.)
A	37.7 ± 0.8	0.12 ± 0.05	53.1% $BaSO_4$, 23.3% $NaNO_3$, 11.9% Na_2SO_4, 11.7% Fe and Co insoluble species
B	40.3 ± 0.3	0.28 ± 0.07	100% $NaNO_3$
C	40.8 ± 0.1	nd	100% $BaSO_4$

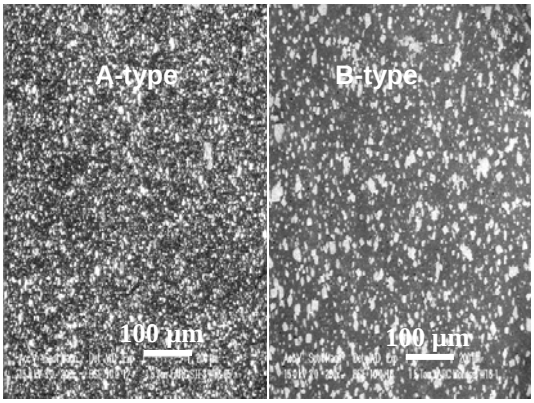

Fig. 1. ESEM observation of sample A (left) and sample B (right) before leaching (backscattered electrons mode).

From ESEM pictures, one gets a qualitative picture of the homogeneity of the incorporation as well as the granulometry of embedded particles. Size distributions of particles have also been quantified by laser granulometry technique, after a toluene extraction of incorporated salts.

A-type shows a bimodal grain distribution centered at 1 and 10 µm, attributed respectively to $BaSO_4$ and $NaNO_3$ particles, which are the major species embedded in A-type. B-type shows a monomodal distribution centered at 20 µm, corresponding to $NaNO_3$ particles. C-type shows a monomodal distribution centered at 1 µm corresponding to $BaSO_4$ particles.
Size differences of $NaNO_3$ particles in A- and B-types are due to the fact that evaporation flow in the extruding machine was fixed whereas the ratio soluble to unsoluble salts was varying in the precursory sludges. This is confirmed by the residual amount of water measured presented (Table 1) and the crystallographic states of particles observed with ESEM at higher magnification scales.
In A- and C-types, the granulometry of $BaSO_4$ particles measured to 1 µm by ESEM as well as laser granolumetry technique can be reduced up to about 200 nm after ultrasonic treatment. This is a clear evidence of the agglomeration of $BaSO_4$ particles in BWP produced by extrusion.

RESULTS

Sorption tests

To illustrate the role of salts solubility against water uptake, water sorption experiments have been undertaken. A sorption balance with controlled relative humidity (RH) has been used on about 100 mg of pristine materials, at the imposed temperature of 298K. Each point has been obtained after the stabilization of water sorption, thanks to a software control of sorption cycles.

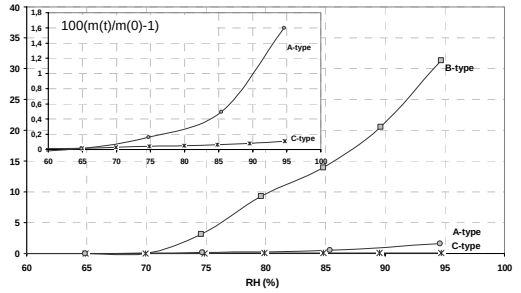

Fig. 2. The water sorption isotherms of the three types of BWP.

The fig. 2 shows that the B-type BWP is able to sorbe twenty times more water than A-type and two order of magnitude more than C-type BWP. This effect relies in the hygroscopic nature of incorporated salts. B-type sorption behavior can be deeper analyzed thanks to the activity of a $NaNO_3$ saturated aqueous solution (0.732) and the availability of these salts in the hydrophobic matrix (salts granulometry and diffusive membrane effects). This has been verified with water sorption experiments performed on another BWP, containing 30% of $NaNO_3$, on one hand and with water sorption experiments on pure $NaNO_3$ and $BaSO_4$ salts on the other hand.
These experiments confirm the role of the incorporated salts solubility in the BWP water uptake capacities in a thermodynamic balance approach.

Leaching experiments

Two aliquots issued from each BWP type have been settled individually in cylindrical polypropylene flasks, so that the height of materials was close to 1 cm.
Pure water, obtained by milliQ filtration, was used for all the leaching experiments. The volume was set to 20 cube centimeters (cc) at short stage of leaching (before day 100) and 50 cc at the longer ones. Such a way, the water activity stays very close to 1.0. The renewal of leachant was periodically performed by complete removal of the leachant and drying of the material surface. The leaching experiments have been undertaken at the temperature of 298K.
Water uptake is monitored by weighting of the dried material during the leachant renewal sequence, and ionic releases (not shown here) are monitored by flame photometry for sodium and potassium ions and ionic chromatography for nitrates and sulfates ions. All the data presented here are averaged. One observes that the discrepancy between two aliquots decreases from about 80 % at first stages of leaching to values lower than 20% at longer stages (over 100 days). This is due to a higher dependence in surface states of aliquots at the beginning of the leaching.
The fig. 3 compares the kinetics of water uptake for the three BWP types. Data have been normalized by the inner surface area of flasks (13.6 cm^2). Ionic species releases are not shown here, but the most labile species (sodium and nitrates) follow a kinetic similar to the one of water but one order of magnitude lower. For type C BWP, since $BaSO_4$ is hardly soluble, the release of ionic species was barely detected.
In fig. 3, A-type BWP uptakes much more water than B-type, whereas its content in soluble species (sodium sulfate and sodium nitrate) is much lower (13 % against 40%). In the same time, C-type BWP, which does not contains any soluble salts, shows its capacity to sorbe water. Furthermore, at shorter stages, its water uptake is similar to the one of B-type, but at longer stages,

the kinetics of water uptake becomes similar to the one of A-type.

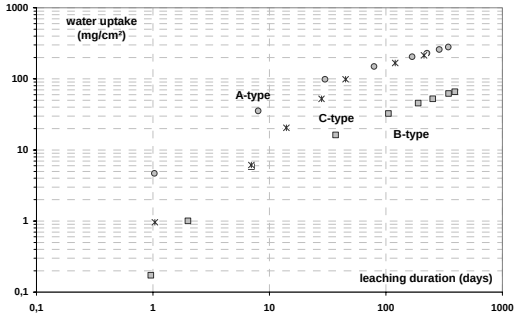

Fig. 3. Comparison of water uptake kinetics for BWP A to C type (mg/cm²).

^{1}H CPMG NMR experiments

To investigate the paradoxal effect presented previously, which is an unexpected impact of insoluble species on water uptake kinetics, NMR ^{1}H experiments have been undertaken with a Minispec Brucker 45 MHz spectrometer. A CPMG sequence has been used [4,5]. Such a way, one gets the total transverse magnetization as a function of acquisition time (fig. 4).

Leaching tests have been performed directly in NMR tubes, with a similar procedure than the one described previously (multiple aliquots, procedure for leachant renewal, 1 cm height in the tube). Here, the tubes inner surface area was 0.503 cm².

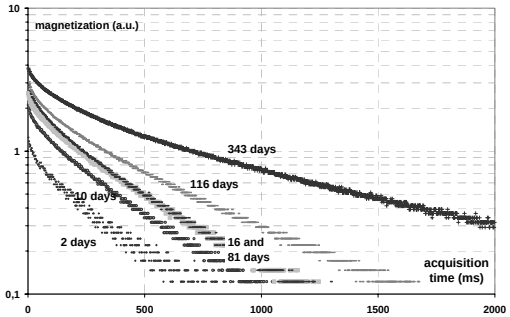

Fig.4. The evolution of ^{1}H-T2 relaxation spectra as obtained with CPMG sequence on B-type BWP leached in situ in NMR tubes at various stages.

Parameters of CPMG sequence have been fixed so that to blind the relaxation of the bitumen matrix hydrogen. The total magnetization has been calibrated against a fixed water volume and one gets a linear equivalence of 200.807 magnetization count per mL of H_2O ($R^2 = 1$). A correction has been applied to subtract the effect of free water present at the top of NMR tubes, even if samples were dried before NMR measurements. In the separated leachants, T2 is varying from 2.0 to 2.5 s, which values are slightly lower than the one of pure water, due to the presence of paramagnetic impurities in the released salts.

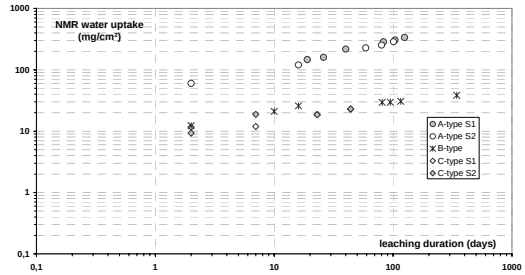

Fig. 5. The water uptake kinetics as observed with ^{1}H NMR, after treatment of CPMG spectra. Several aliquots of same BWP type are presented here for reproducibility evaluation.

The fig. 4 shows the variation against leaching duration of T2 relaxation spectra for one B-type aliquot. The y-scale extrapolated at 0 ms indicates the total amount of water present in the porous zone. The signal decreases proportionally to the quenching of water relaxation, first occurring in the smaller pores. A multi-exponential deconvolution allows the estimation the volume fraction of confined water population as well as the associated T2. We paid a great attention on the physical reliability of this mathematical treatment (minimal number of exponentials used, sufficient distance of calculated T2 in converged calculations, good statistics against chi² test).

The fig. 5 shows the water uptake kinetics as extracted from the total magnetization measurement and numerical treatment. These results are directly comparable in a good agreement with those presented on fig. 2 and confirm the behavior of A- and B-types. Unfortunately, at the present time, some data were missing on C-type materials to confirm the acceleration of water uptake above 50 days.

Fig. 6 to 8 show for each type of material the repartition of the porous volume as observed after a mathematical deconvolution of CPMG spectra. At each step of the leaching, one gets 3 or 4 T2 (depending of BWP type) to be associated to a distinct water population in the porous zone. For each material and water population, the calculated T2 value is found as a constant against time plus or minus a given error bar. The reproducibility evaluation has also been monitored on series A and C, with two aliquots, leading either to complementary data (A-type) either to error bars (C-type), depending whether

measurements were performed with a time lag or without.

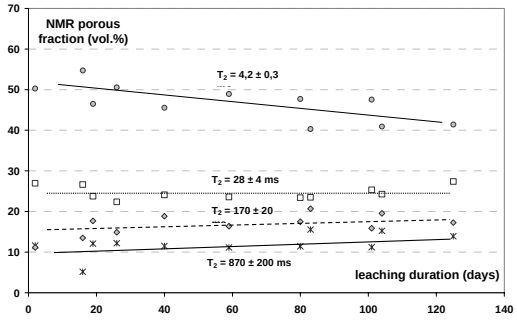

Fig. 6. The volume fraction occupied by confined water as a function of leaching duration in A-type BWP. Lines are guide for the eyes.

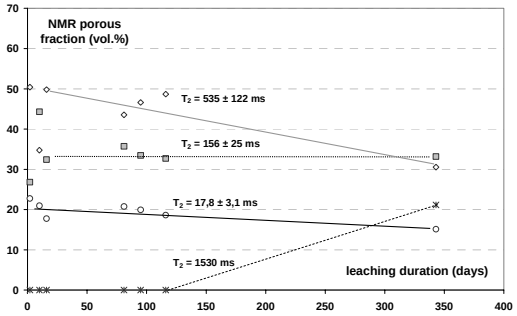

Fig. 7. The volume fraction occupied by confined water in leached B-type BWP.

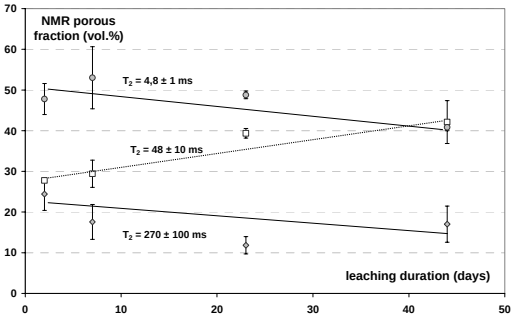

Fig. 8. The volume fraction occupied by confined water in leached C-type BWP.

The fig. 6 to 8 show that the main contribution of porous fraction is due to highly confined water in A- and C-types BWP (small T2 values). In contrast, in B-type material, the major contribution to total porous volume is due to the bigger pores. The conclusion is that water uptake in industrial-like BWP is controlled at first order and at short and medium stages of leaching by the smallest incorporated species, probably associated with small and insoluble salts.

The calibration of pores sizes against T2 value is not direct yet, because of the presence of various saline species, soluble or not, in pore water. The evolution of pore populations follow the global trend of a decrease of the most confined water, which is an indirect evidence of the swelling of the porous zone with time.

CONCLUSION

These results put into evidence the effect of insoluble salts in the water uptake kinetics. This effect may be attributed to a percolation mechanism enhanced with the presence of small and hydrophobic salts. This is really new but has to be deeper evaluated before updating long term predictive modeling of the BWP leaching, since we have not at that time correlated this effect with the salts release kinetics.

Low field NMR technique allows an indirect quantification of pore populations and associated volume fractions evolution during leaching. Further endeavors have to be provided to link T2 values to explicit pore sizes, and for comparison with direct ESEM observations. To improve the description of the porous zone and its impact on the leaching kinetics, the use of ^{1}H and ^{23}Na NMR imaging techniques and SANS experiments are planned.

ACKNOWLEDGEMENTS

Authors want to thank warmly Agnès Barré, Isabelle Felines, Karine Ressayre, Nadège Mialon and Cyril Roussignol for their respective contribution to BWP production, ESEM observations, solid and solution analysis, and laser granulometry measurements.

REFERENCES

1. B. Gwinner, J. Sercombe, I. Félines and F. Adenot, *J. Nucl. Mat.* **349** (2006) 107-118
2. J. Sercombe, C. Tiffreau, B. Gwinner and F. Adenot, *J. Nucl. Mat.* **349** (2006) 96-106
3. *Proc. of Int. Workshop on the Safety and Performance Evaluation of Bituminization Processes for Rad. Wastes*, Prague, 1999.
4. H.Y. Carr and E.M. Purcell. *Phys. Rev.* **94** (1954), 630
5. S. Meiboom and D. Gill., *Rev. Sci. Instrum.* **29** (1958), 688